

Original Article

Design of Corona-shaped 2X2 UWB- MIMO antenna using Characteristic Mode Analysis

Ankireddy Chandra Suresh¹, T. Sreenivasulu Reddy²

¹Research Scholar, Department of Electronics and Communication Engineering, SVUCE, SV University, Tirupathi, A.P, India.

²Professor, Department of Electronics and Communication Engineering, SVUCE, SV University, Tirupathi, A.P, India.

¹ archandu.suresh@gmail.com, ² mettu86@yahoo.co.in

Abstract - A Corona Shaped 2X2 Multiple Input Multiple Output (MIMO) UWB antenna with dimensions of $36 \times 18 \times 1.6 \text{ mm}^3$ ($0.32\lambda \times 0.16\lambda \times 0.0144\lambda$) is proposed for wireless communication. A novel designing procedure is achieved through characteristic mode analysis (CMA). CMA is used to analyze the physical structure of an antenna and its dominant mode. The proposed UWB-MIMO antenna comprises two monopole circular-shaped radiators that act as radiating elements to the MIMO antenna to achieve UWB operation. The designed antenna achieved isolation greater than 18 dB, and return losses are $S_{11} < -10 \text{ dB}$ in the entire frequency spectrum (3-15GHz), including UWB, X-band (8-12GHz) and ITU (10.7 to 11.7 GHz) (12.75 to 13.25 GHz). Isolation is maximized by inserting T-shaped stubs into the ground plane. The diversity parameters such as ECC, DG, Mean Effective Gain, and CCL meets the requirements of UWB applications. The designed antenna achieves 150.9% impedance bandwidth, the radiation efficiency is 72.5%, and the gain is 4.2dB. The designed antenna is fabricated and tested for validation. There were very favourable agreements between the simulated and tested results.

Keywords — UWB-MIMO, CMA, Isolation, Mean effective Gain, Dominant Mode.

I. INTRODUCTION

The announcement by the Federal Communication Commission (FCC) of an unlicensed frequency spectrum ranging from 3.1GHz to 10.6GHz sparked a surge in interest in UWB antenna research. Because UWB has tremendous advantages like low interference, high data rates in the short range, and allows for reliable communication systems [1-4]. But UWB technology also suffers from multi-path fading and low power capabilities. The future trademark of wireless communication is MIMO (Multiple Input and Multiple Output) because it offers high data rates and low power. As a result, the combination of UWB and MIMO technology reduces the problem of fading and multipath, increasing transmission capacity and gain in wireless communication [5]. The mutual interaction problem occurs due to increasing the compactness of the MIMO by placing more antenna elements in a small space. The drawback of UWB-MIMO is

that it suffers from a coupling between the elements. This mutual coupling affects the diversity performance of MIMO and degrades the reliability of wireless communication [6].

There are numerous methods for reducing mutual coupling, such as space diversity, adding decoupling networks, defected ground structures, placing parasitic elements, EBG (electromagnetic band gaps), polarization diversity, and metamaterials [7-9].

Placing different types of stubs not only reduces mutual interference but also reduces the diversity gain and radiation efficiency, which causes less reliability in UWB-MIMO antenna applications [10]. A T-shaped slot is etched on the ground of MIMO and designed with small dimensions of radiating elements [11]. The UWB-MIMO antenna is composed of two Planer Inverted-F-antenna (PIFA) and a metallic strip. An Extra folded resonator is inserted. The PIFA design not only increases isolation but also provides good pattern diversity [12]. A small size Uniplanner Electromagnetic band gaps (UC-EBG) are used along two circular monopole radiators to enhance the isolation [13]. In 2X2 MIMO, the patch antennas have a superstrate layer, and an array of UC-EBG miniaturization structures are inserted on the top of each radiator to increase the performance of diversity parameters [14]. The magnetic metamaterial and substrate-integrated split-ring resonators are shared as a common substrate in two radiators. Magnetic fields are stagnated in the common substrate due to the near-field effect and mutual coupling due to the nature of negative permeability (SI-SRR) [15]. The metamaterials are made of dual-resonant meta-atoms and triple-resonant meta-atoms (TRMA) and arranged in either a Z- or an S-shape. The TRMA offers a negative permittivity that eliminates the mutual coupling [16]. In each radiator of the MIMO system, the mutual coupling is eliminated by generating an 180° phase shift electric field inversion [17]. To maximise isolation, reduce channel capacity losses, and improve diversity characteristics, the metamaterial unit cell structure is placed between two MIMO radiators [18]. The MIMO antenna is comprised of two radiating elements and is symmetrically placed, and isolation is enhanced by adding



split rectangular loop resonators along with long stubs in between the two radiators [19]. A complementary Splint ring resonator (CSRR), symmetrical Splint ring resonators (SSRR), and S-shaped slots are used to get high isolation in ultra-wideband circular Microstrip patch antennas [20]. To achieve good port isolation, the parasitic inverted neutralization stubs are placed in between fractal-shaped MIMO elements [21]. The high isolation is obtained in UWB meandering monopoles by the combination of two inverted L-shape slots and two L-shape stubs with an etching slot on the ground [22]. Better diversity performance and bandwidth improvement are obtained in the UWB Yagi-Uda MIMO antenna by using yagi miniaturization. The space diversity method produce compactness in MIMO [23]. To improve isolation in 2X2 MIMO antennas, L-shaped slots and narrow slots are used [24]. A wideband neutralisation line with a decoupling stub is inserted in between 2 symmetrical radiating elements to enhance isolation along with diversity performance [25]. The spatial diversity, polarization, and pattern diversity methods are implemented in a 3-staircase-shaped UWB-MIMO antenna to maximise the isolation of more than 25dB in UWB [26]. The FSS slotted Y-shape, and L-shaped decoupling on the ground enhance the isolation and reduce mutual coupling. The square spiral acts as the parasitic element to optimize the impedance [27].

Two similar types of radiators are symmetrically arranged so that the radiation direction is opposite to the orientation and cancel each other. This system did not use any special decoupling method but achieved better isolation [28]. The MIMO antenna is composed of two strip lines fed by staircase-shaped radiating elements, and an isolating metallic strip is placed between them to reduce the envelope correlation coefficient by up to 0.163, increase efficiency up to 90%, and provide good separation of more than 20dB. The T-shaped slot and etched line slots in the ground produce better impedance matching isolation and also achieve the omnidirectional radiation pattern [29]. The antenna consists of a semi-circular and semi-square ring with a curved radiating element to create a defective ground. To improve isolation and bandwidth, an extended ground stub is added [30]. Dual-polarization is produced in the MIMO system by two different radiating elements and different feeding systems used to achieve good radiation performance in the MIMO system [31]. In the MIMO antenna system, a metal strip acts as a decoupling structure with a triangular slot, resulting in the isolation of more than 20dB. The MIMO is made up of two P-shaped. Isolation is improved even more with a suspended stripline in the ground plane. The antenna is made up of two truncated corner square patched radiators and parasitic metallic plates that are arranged in such a way that mutual coupling is minimized for WLAN applications [32]. For reliable wireless communication, the isolation in the UWB-MIMO system must be improved. Characteristic mode analysis is a well-known systematic design approach.

The orthogonal currents in a perfect electric conductor explain the fundamental characteristic mode theory [33-34].

However, the antenna design work presented above is not up to the mark. There is a good chance that placing antenna elements in orthogonal modes and using defective ground systems will improve isolation. The space diversity method is used in conjunction with a systematic design approach and characteristic mode analysis to achieve high isolation. We created a 2X2 UWB-MIMO antenna using this method, which uses a novel methodology to achieve high isolation and better diversity performance than ECC, DG, CCI, and MEG.

Two circulars (Corona)-shaped monopoles are used in the proposed work, with a T-shaped decoupling stub structure is placed on the ground. The characteristic mode theory is used to examine physical insight and the dominant model.

II. DESIGN OF CORONA SHAPED 2X2 UWB-MIMO ANTENNA

CMA is used to design the proposed antenna with $\epsilon_r = 4.3$ and $\tan\delta = 0.002$. The designed UWB-MIMO antenna is made up of two symmetrical monopole antennas that are placed symmetrically on the FR-4 substrate. The dimensions of a designed antenna are 36x18x1.6 mm³. Each circular radiator is composed of seven small circular-shaped patches (bubbles), which are added around the circumference of the circular patch radiator. The designed antenna uses a space diversity method to achieve good diversity performance. The distance between two radiators from centre to centre in this antenna is 20 mm to maximise isolation. A T-shaped stub on the ground with compact dimensions improved the isolation and is depicted in Fig.1.

Decoupling in the shape of T Stubs are used to improve impedance bandwidth and isolation. The feed width is 1.5mm, and the circular radiator radius is 4mm. It's made to resonate at three UWB frequencies: 2.9 GHz, 5.8GHz, and 9.6 GHz. The designed values are shown in Table.1.

Table 1. The corona shaped 2X2 UWB MIMO antenna Dimensions is listed. (unit mm).

r	Lf	Wf	Ls	Ws
4	4	1.5	18	36
d1	d2	L1	L2	L3
20	1.4	3	12	10
Lg	W3			
3	3			

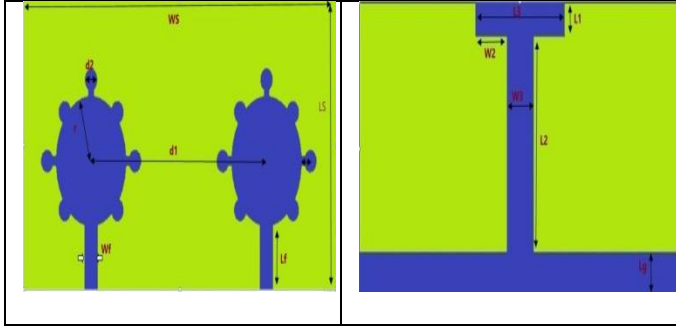


Fig.1. Corona Shaped 2X2 UWB-MIMO Antenna

A. Characteristic Mode Theory for 2X2 Corona shaped MIMO Design

The characteristics mode theory analyses and measures the resonant modes in perfect electric conductors (PEC) to understand the physical insight into antenna structures [35]. Each characteristic mode (CM) gives the CM metrics as (i) Eigenvalue and (ii) Characteristic Angle. (iii) Modal Importance.

(i) Modal Significance (Ms):

The modal significance of a particular mode is resonated only when $M_s = 1$. This can be derived from the magnitude of weighted Eigenvalues. The M_s can be expressed in terms of eigenvalues

$$MS = \left| \frac{1}{1 + j\lambda_n} \right| \tag{1}$$

(ii). Characteristic Angle:

The characteristic angle where it crossed 180° is called the characteristic mode.

$$\Phi = 180^\circ \left(1 - \frac{1}{\pi} \arctan(\lambda_n) \right) \tag{2}$$

(iii) Eigen Value:

The eigenvalue $\lambda_n = 0$ at one particular frequency and that frequency is treated as the resonant frequency of that particular mode.

The antenna design using characteristic mode analysis is more effective and efficient than the antenna design using the trial and error method. The Eigenvalues are calculated with the help of a matrix, which is called the method of the moment matrix.

$$[I]J_n = \lambda_n [R]J_n \tag{3}$$

$$[Z]J_n = [R]J_n + [I]J_n \tag{4}$$

Here, R and I are real and imaginary parts of the moment impedance matrix, λ_n is the Eigenvalue, and J_n is the Eigen current, respectively. Solving the above (3) and (4) equations for a mode of operation. The Modal significance of characteristic mode is

$$J = \sum_{n=1}^N C_n J_n \tag{5}$$

Where C_n is mode coefficient, by solving the above equations

$$|c_n| = \frac{V_n}{1 + j\lambda_n} = |V_n| M_s \tag{6}$$

The corona shaped 2X2 UWB-MIMO antenna is analysed by using a multilayer solver or integral solver (CST-2018) without applying excitation and feed. The designed antenna produces different characteristic modes, each mode having modal significance, Eigen Values, and characteristic angles, respectively. The modal significance and characteristic angles of the designed antenna are depicted in Fig.2.

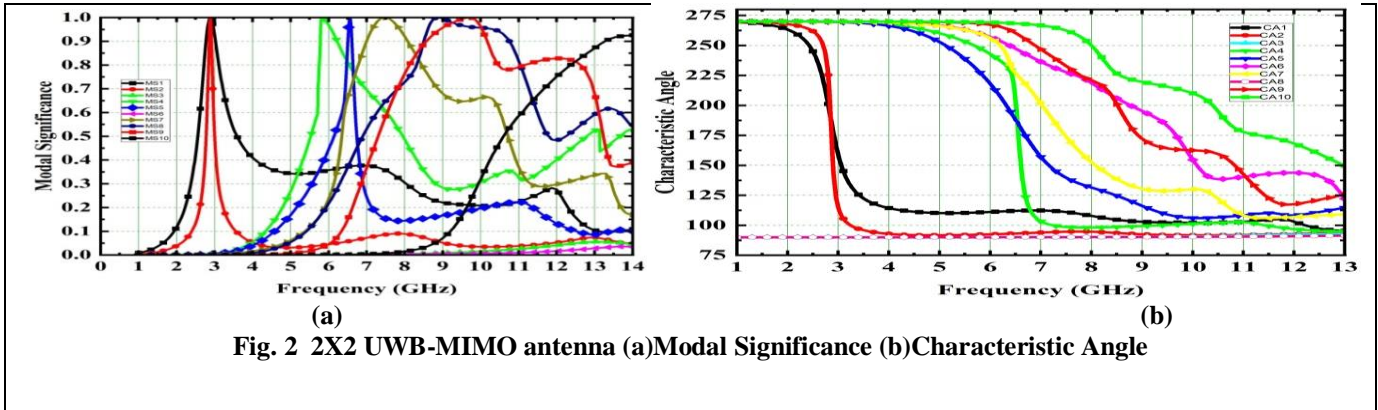


Fig. 2 2X2 UWB-MIMO antenna (a) Modal Significance (b) Characteristic Angle

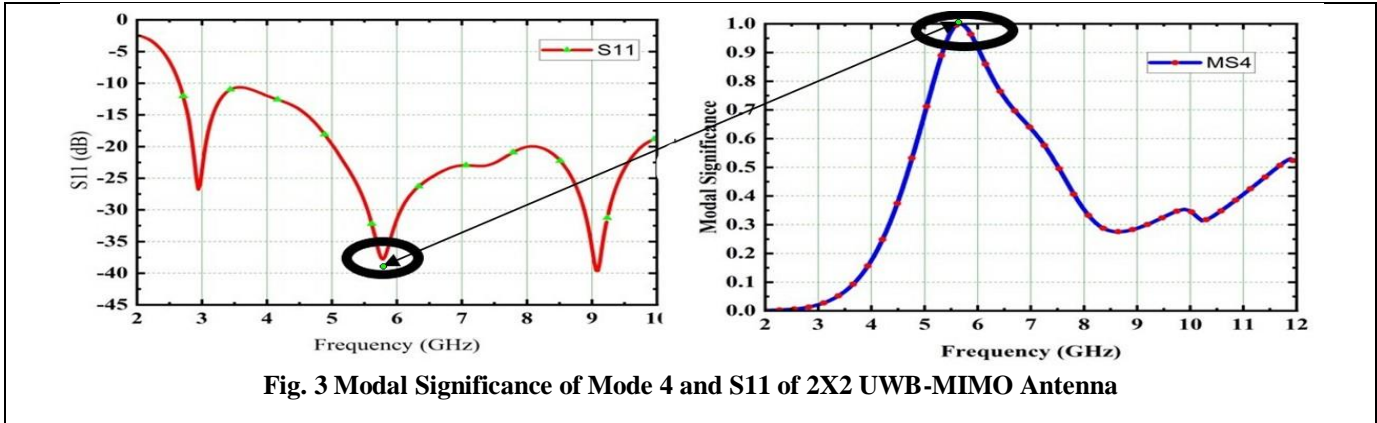


Fig. 3 Modal Significance of Mode 4 and S₁₁ of 2X2 UWB-MIMO Antenna

The designed antenna produces 10 characteristic modes. Only five of the ten modes are significant at their respective frequencies. The CM1 and CM2 are strongly resonated at 2.8 GHz and treat this mode as non-dominant because it does not fall within the UWB range (3.1GHz–10.6GHz). The CM3, CM6, and CM10 did not reach the magnitude one ($M_s = 1$) in the modal significance graph, so these modes are useless. The remaining modes, CM4, CM5, CM7, CM8, and CM9, are useful [41]. In their modal significance graphs, the above-mentioned modes' modal significances approach magnitude one. But out of the five modes, three modes, CM5, CM7, and CM8, did not act as dominating modes because the radiation characteristics of mode 5, mode 7, and mode 8 are not good.

The remaining two modes, CM4 and CM9, are acting as dominant modes and their corresponding resonating frequencies are 5.8GHz and 9.6 GHz, respectively. The frequency of 5.8GHz is useful for WLAN applications. The modal significance of CM4 and S₁₁ parameters is that they resonate at the same frequency at 5.8GHz. Hence, this mode is called the dominant mode and is shown in Fig.3. The characteristic mode current (CMC) distributions of CM1, CM4, and CM9 are depicted in Fig. 4, Fig. 5, and Fig. 6, respectively. The current densities of UWB-MIMO antennas at various frequencies are shown in Fig.7.

III. RESULTS OF DESIGN OF CORONA SHAPED ANTENNA

The Corona Shaped antenna is accomplished using the systematic design approach (CMA). The designed antenna prototype is fabricated and tested. One port is connected to a Vector Network Analyzer (N5230A) while measuring the S-parameters, and the other port is assigned to a matched load of 50Ω load. The S₁₁ is very similar to S₂₂, and simulated values are compared with measured values. The return losses S₁₁ and S₂₂ are below -10dB, and isolation parameters S₂₁ and S₁₂ are below -18dB in the entire UWB. The fabricated prototype of the corona shaped antenna is depicted in Fig. 8. The comparison of S₁₁ simulated and measured is depicted in Fig.9. The comparison of isolation parameters is depicted in Fig.10. The designed antenna is placed in an anechoic chamber to measure the radiation patterns, as shown in Fig.11. The radiation pattern co-polarization and cross-polarization of the E-pattern, as shown in Fig.12. At 2.8GHz, 5.8GHz, and 9.6GHz, the radiation patterns were measured. The first radiator is excited at port one, and port two is matched with a 50 Ω load for measuring radiation patterns. With the help of DRH20, the radiation patterns are measured in an anechoic chamber. The Radiation patterns are measured at different frequencies in the UWB spectrum. Co-polarization and cross-polarization of E-Plane and H-plane measures for designed corona shaped 2X2 UW MIMO antenna. This radiation patterns are good. The radiation efficiency achieved is 72 % and depicted in

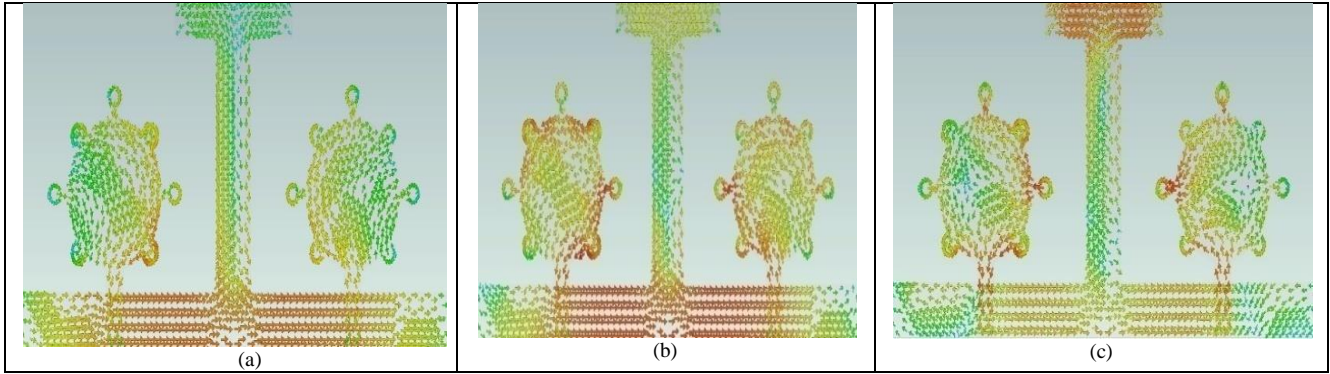


Fig. 4 Distributions of CMC in 2X2 Corona shaped Antenna for Mode1 at (a)2.8GHz (b)5.8GHz (c)9.6GHz

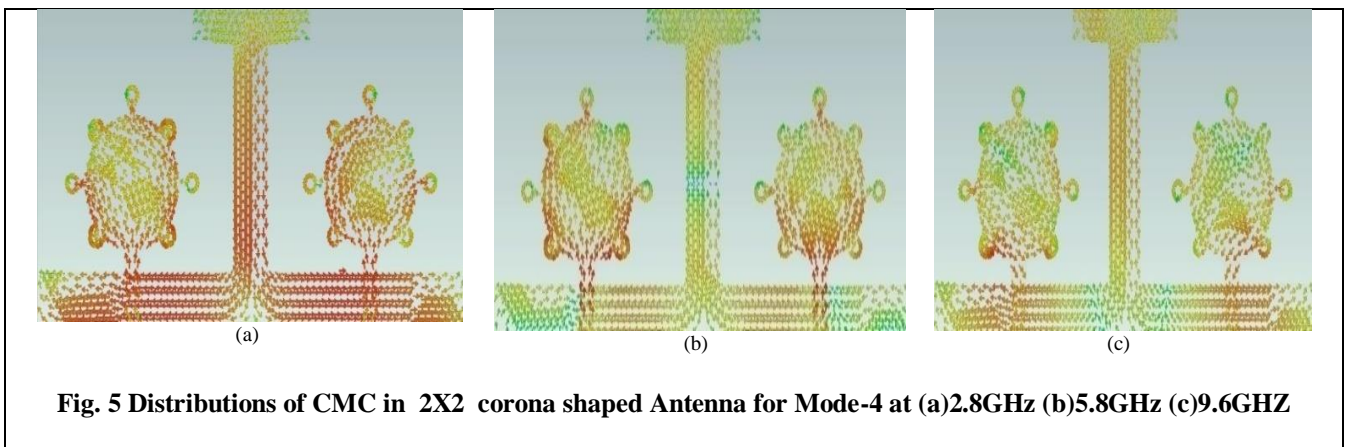


Fig. 5 Distributions of CMC in 2X2 corona shaped Antenna for Mode-4 at (a)2.8GHz (b)5.8GHz (c)9.6GHz

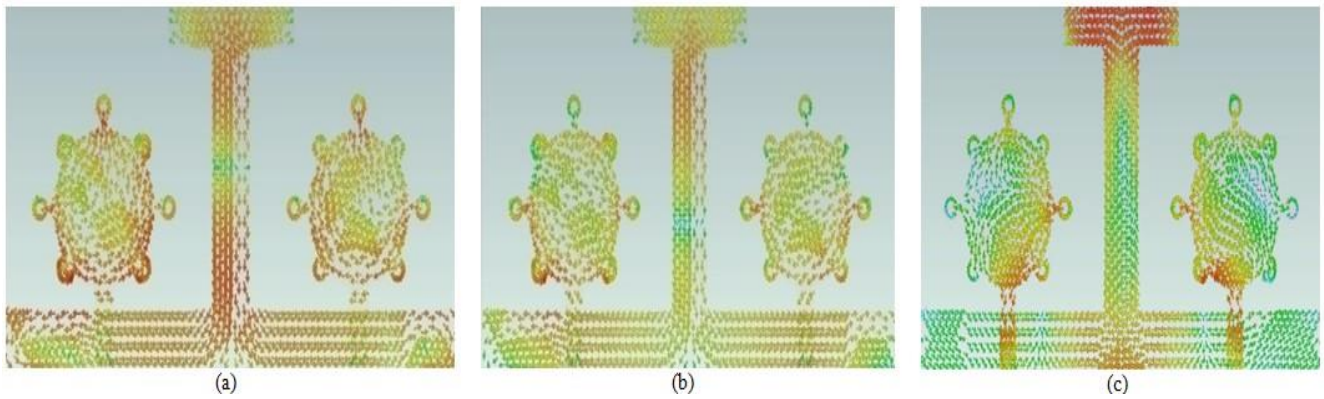


Fig.6 Distributions of CMC in 2X2 Corona shaped Antenna for Mode-9a at (a)2.8GHz (b)5.8GHz (c)9.6GHz

The radiation patterns show that this antenna is suitable for the reliable communication link. The radiation characteristics of the designed corona shaped 2X2 UWB MIMO antenna is good and meets the requirements of UWB, X-band and ITU bands.

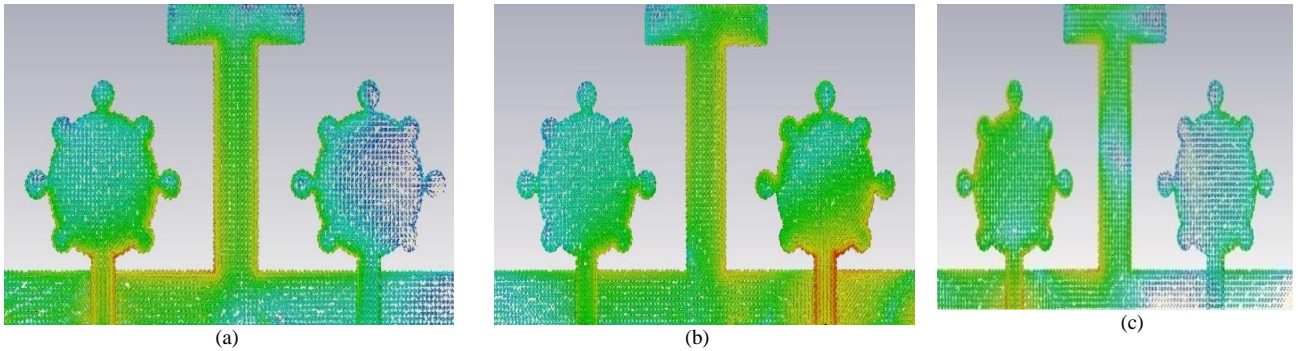


Fig.7 Surface Current densities of 2x2 UWB-MIMO Antenna at (a)2.8GHz (b)5.8GHz (c)9.6GHz

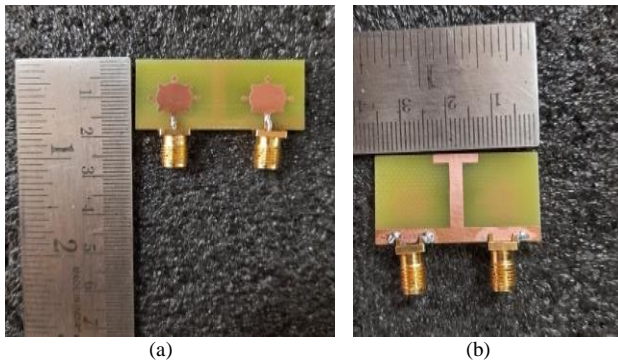


Fig.8 Prototype of Designed antenna (a) Top View (b) Bottom View

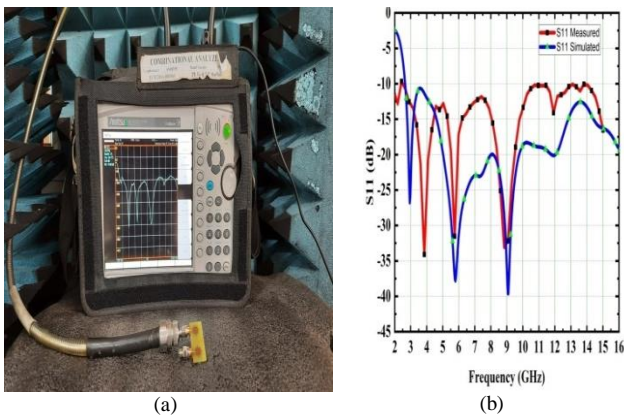


Fig. 9 (a) S_{11} measured (b) S_{11} measured with simulated Values

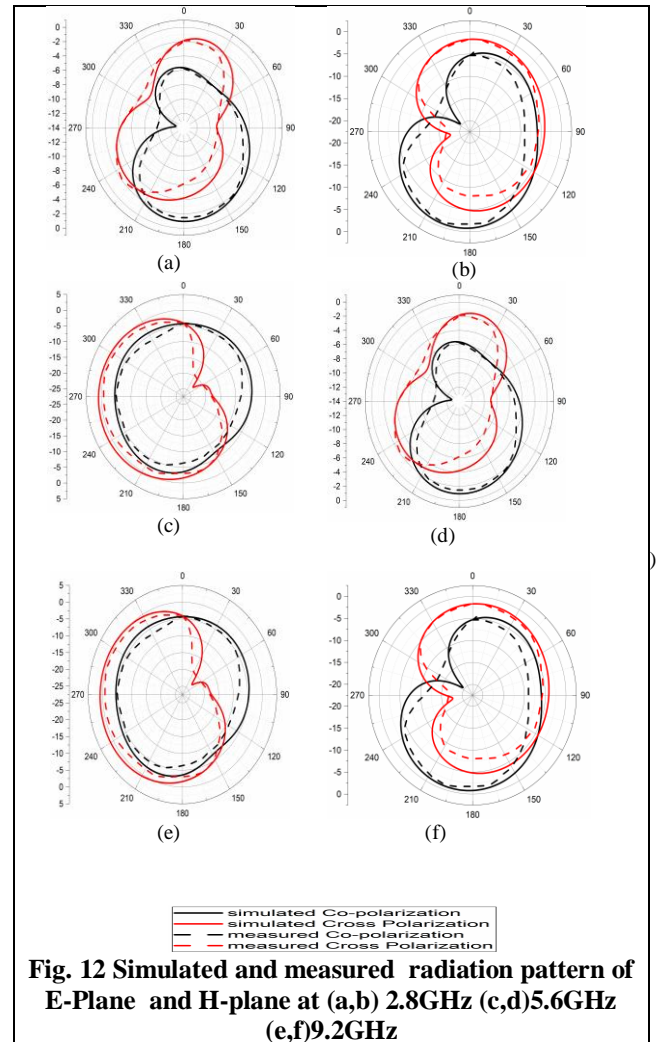
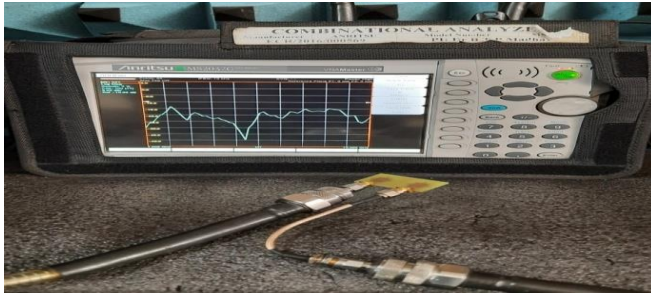
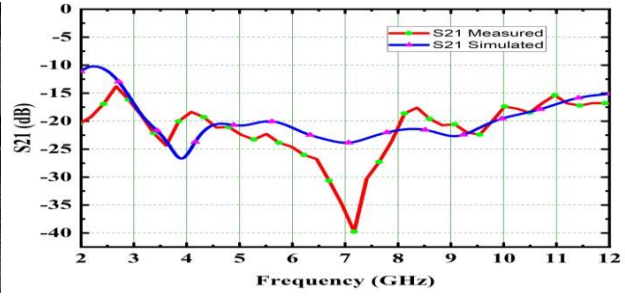


Fig. 12 Simulated and measured radiation pattern of E-Plane and H-plane at (a,b) 2.8GHz (c,d)5.6GHz (e,f)9.2GHz

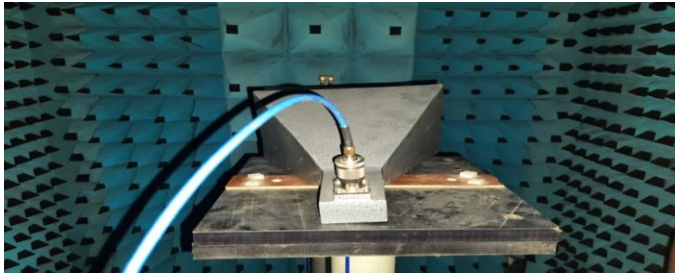


(a)

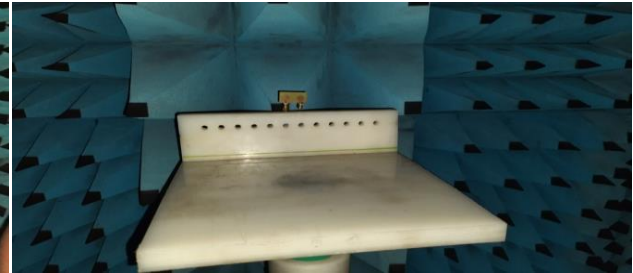


(b)

Fig. 10 (a) S21 measured (b) S21measured with simulated

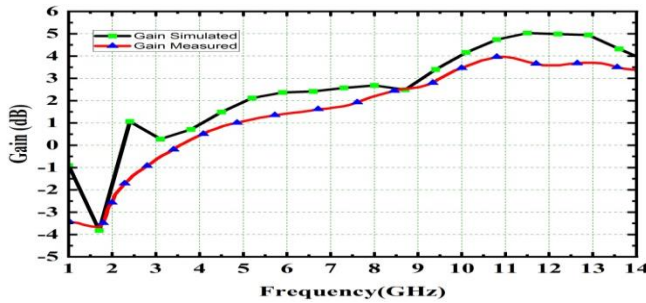


(a)

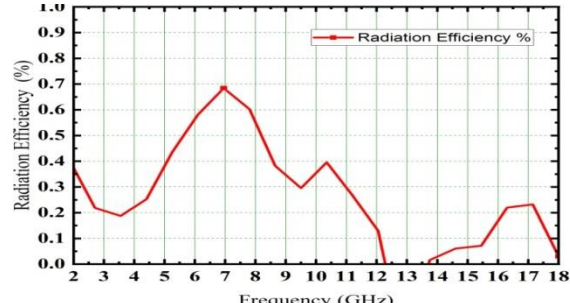


(b)

Fig. 11 Measurement of the radiation pattern in an anechoic chamber.



(a)



(b)

Fig. 13 (a) Comparison of Gain simulated with measured (b) Radiation efficiency.

A. Diversity Performance of Corona Shaped 2X2 UWB-MIMO Antenna

The envelope correlation coefficient, diversity gain, mean effective gain, channel capacity, and TARC are the MIMO antenna's characteristics. These parameters should be within acceptable limits; otherwise, MIMO performance will be poor and unsuitable for secure wireless communication. As a result, using MATLAB code, the above diversity parameters are calculated and plotted, as well as verified with measured values.

B. Envelope Correlation Coefficient (ECC)

One of the key performances of MIMO is the envelope correlation coefficient (ECC). It describes how the elements of MIMO are decoupled [37]. In MIMO, the ideal case of ECC is zero, but practically it is not possible, so the

acceptable value of ECC is < 0.5. In the 2X2 MIMO system, the ECC is expressed in terms of S-Parameters is

$$ECC_{km} = \frac{|S_{kk}^* S_{km} + S_{mk}^* S_{mm}|^2}{(1 - |S_{kk}|^2 - |S_{mk}|^2)(1 - |S_{mm}|^2 - |S_{km}|^2)} \quad (7)$$

Here k=1,m=2. The graph of ECC for the 2X2 corona shaped antenna is depicted in Fig.14. Its value is less than 0.0008 in the UWB spectrum.

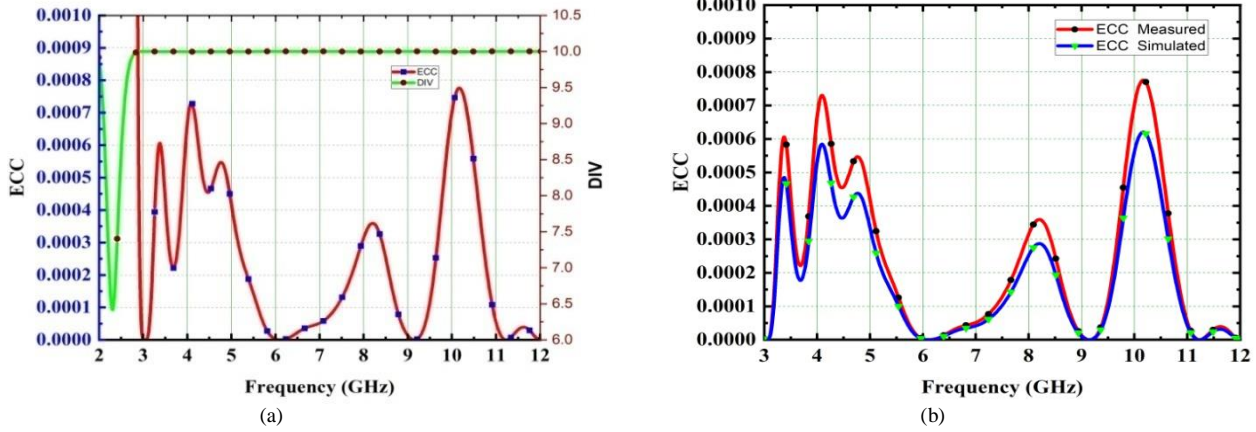


Fig. 14 (a) ECC with DG (b) ECC

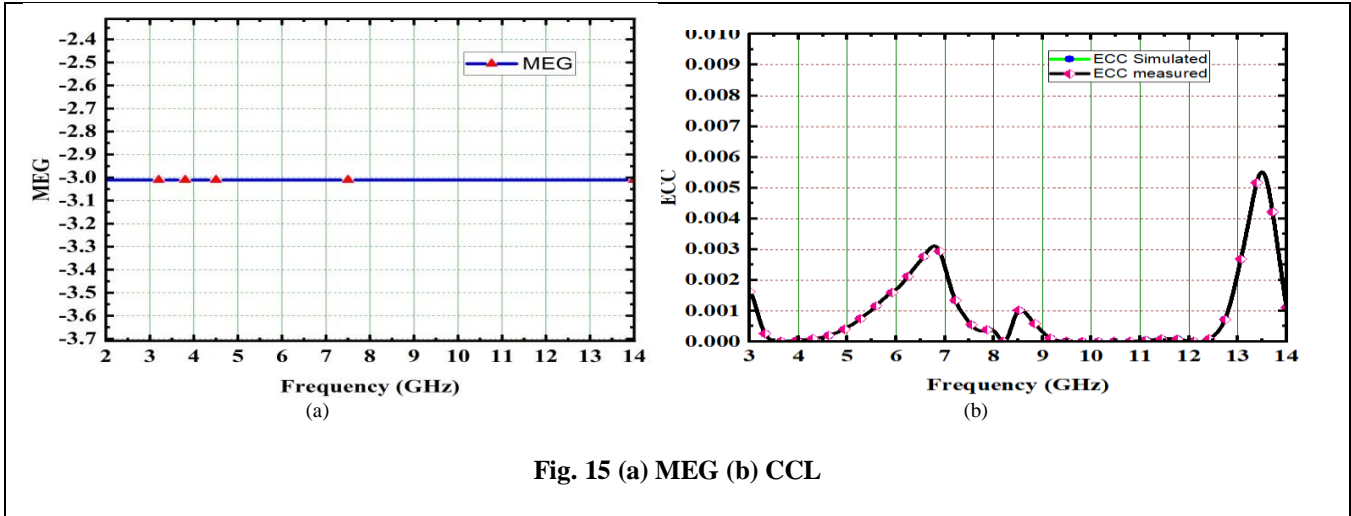


Fig. 15 (a) MEG (b) CCL

C. Directive Gain

The designed 2X2 UWB-MIMO antenna uses diversity techniques to increase the isolation. The diversity gain of the corona shaped antenna is explained using equation (8). A MIMO antenna with good diversity performance should have a diversity gain of around 10dB. The Corona Shaped antenna achieved 9.998dB and is depicted in Fig.14(a).

$$DG = 10\sqrt{1 - ECC^2} \tag{8}$$

D. Mean effective gain

The MEG is also one of the characteristics of the MIMO. In a MIMO system, the MEG is defined as the ratio of average received power to average incident power by a microstrip patch antenna. For the measurement of MEG, it is always taken as a reference as an isotropic antenna.

$$MEG = \int_0^{2\pi} \int_0^\pi \left[\frac{X_{PR}}{1+X_{PR}} M_\theta(\theta, \phi) N_\theta(\theta, \phi) + \frac{1}{1+X_{PR}} M_\phi(\theta, \phi) N_\phi(\theta, \phi) \right] \sin \theta d\theta d\phi \tag{9}$$

where M_θ and M_ϕ are patterns of power in the MIMO antenna system. Generally, in the MIMO antenna system, the MEG is always less than -3dB. In the proposed 2X2 antenna, MEG is measured and got -3.1dB and depicted in Fig.15.a.

E. The Channel Capacity loss

The CCL is also a key matrices factor in the MIMO system. The minimum acceptable limit of CCL in the MIMO system is 0.4 bits/s/Hz. The simulated and measured values of CCL are shown in Figure 15 (b). The corona shaped MIMO achieved a CCL value of 0.299 bits/s/Hz over the spectrum.

Table.2 Comparison of corona shaped 2X2 MIMO with existing Models

Ref	Geometry	Isolation Method	B.W(%)	Isolation (dB)	ECC	Effi (%)	Gain (dB)
[25]	Circular monopoles	Naturalization Lines	93.82	<-22	0.1	90	5.5
[38]	Coplanar staircase shape	Back-Back	115	<-19	0.2	90	5.5
[27]	FSS based cuboid	T-shaped Stubs	109.28	<-20	<0.5	60	---
[28]	QSF	Opposite oriented Radiators	133.23	<-20	<0.25	88	6.5
[29]	Strip line-fed staircase	metal-strip in-between	109.28	<-20	0.1	90	5.2
[31]	Circular+Square) ring/2	Polarization diversity	111.42	<-15	0.1–0.2	75	3.5
[32]	Distinct PIFA's	shorting strips	129	<-15	0.08	58	3.39
[33]	P-shaped monopole	triangular meshed strips	131.2	<-20	0.02	---	4.2
[39]	CPW+L-shaped element	inverted L-Stubs	109.5	<-14.2	0.047	72.12	1.6
[40]	Patch+Parasitic element	---	113.7	<-20	0.05	---	5.8
[41]	Square monopole+L-slot	parasitic structures	118.2	<-20	0.004	---	3.32
[42]	Fractal+Contorted feed	Neutralization line+slots	118.18	<-22.5	0.025	50	8.4
Prop	CircularMonopoles	T-Shaped Stubs	150.2	<-18	0.00075	72	4.2

IV. COMPARISONS OF PROPOSED WORK WITH OTHER MODELS

The performance of the designed antenna is compared with that of existing models, and its performance is summarized in Table.2, which includes the performance parameters like Impedance bandwidth, return losses, isolation, ECC, efficiency, and gain. Some MIMO antennas with similar dimensions are designed and discussed in the literature review, but the proposed Corona shaped 2X2 MIMO antenna is the best in terms of impedance bandwidth. The designed antenna achieves a higher impedance bandwidth compared to [25–42].

V. CONCLUSIONS

This 2X2 UWB-MIMO antenna design is well organised with two circular-shaped monopoles with T-shaped stubs to enhance the isolation. Using the proper design method, CMA achieved more than 18dB of isolation. From the characteristics mode analysis, it is found that the dominant mode resonates at 5.8GHz. The radiation efficiency is > 70% , ECC of less than 0.0008, DG is 9.99dB, CCI is 0.29 bits/Hz, impedance bandwidth is 150.99% and

MEG is less than -3.1dB .This antenna is well suited for WLAN applications.

ACKNOWLEDGEMENT

The authors declare that they have no known competing financial interests or personal relationships that could have appeared to influence the work reported in this paper.

REFERENCES

- [1] Yang, L. and G. B. Giannakis, Ultra-wideband communications: An idea whose time has come, IEEE Signal Process. Mag., 21 (6) (2004) 26–54.
- [2] Fontana, R. J., Recent system applications of short-pulse ultra-wideband (UWB) technology, IEEE Transactions on Microwave Theory and Techniques, 52(9) (2004) 2087–2104.
- [3] Zhu, F., et al., Multiple band-notched UWB antenna with band-rejected elements integrated with the elements integrated into the feed line, IEEE Trans. Antennas Propag., 61(8) (2013)3952–3960.
- [4] Li, L., S. W. Cheung, and T. I. Yuk, Compact MIMO antenna for portable devices in UWB applications, IEEE Trans. Antennas Propag., 61(8) (2013) 4257–4264.
- [5] Li, K.; Shi, Y., Wideband MIMO handset antenna design based on a theory of characteristic modes., Int. J. RF Microw. Comput. Aided Eng. 2018,
- [6] Abiodun, O.; Yang, H.; Wu, Y., Enhancing the security of wireless communication with the aid of guard nodes., J. Commun. (11) (2016) 586–591.
- [7] Christos, M.; Michail, M., Space-constrained massive MIMO: Hitting

- the wall of favourable propagation., *IEEE Commun. Lett.* (19) (2015) 771–774.
- [8] Kundu, L., *Information-Theoretic Limits on MIMO Antennas*. PhD. Thesis, North Carolina State University, Raleigh, NC, USA, 2016.
- [9] Qian, K.-W.; Huang, G.-L.; Liang, J.-J.; Qian, B.; Yuan, T., An LTCC interference cancellation device for closely spaced antennas is decoupling., *IEEE Access*, (6) (2018) 68255–68262.
- [10] Iqbal, A.; Saraereh, O.A.; Ahmad, A.W.; Bashir, S., Mutual coupling reduction using F-shaped stubs in UWB-MIMO antenna., *IEEE Access* (6) (2018) 2755–2759.
- [11] Luo, C.-M.; Hong, J.-S.; Zhong, L.-L., Isolation enhancement of a very compact UWB-MIMO slot antenna with two defected ground structures., *IEEE Antennas Wirel. Propag. Lett.*,(14) (2015) 1766–1769.
- [12] Lee, C.H.; Chen, S.Y.; Hsu, P., Integrated dual planar inverted F antenna with enhanced isolation., *IEEE Antennas Wirel. Propag. Lett.*, (8) (2009) 963–965.
- [13] Dabas, T.; Gangwar, D.; Kumar, B.K.; Gautam, A.K., Mutual coupling reduction between elements of UWB MIMO antenna using small size uniplanar EBG exhibiting multiple stopbands., *Int. J. Electron. Commun.*, (93) (2018) 32–38.
- [14] Farahani, H.S.; Veysi, M.; Kamyab, M.; Tadjalli, A., Mutual coupling reduction in patch antenna array using a UC-EBG superstrate., *IEEE Antennas Wirel. Propag.*, (9) 2010) 57–59.
- [15] Liu, Z.-T.; Qu, S.-B.; Wang, J.-F.; Zhang, J.-Q.; Hua, M.; Xu, Z.; Zhang, A.-X., Isolation enhancement of patch antenna array via metamaterial integration., *Microw. Opt. Technol. Lett.*, (58) (2016) 2321–2325.
- [16] Marathe, D.; Kulat, K., A compact dual, triple band resonators for negative permittivity metamaterial., *Int. J. Electron. Commun.*, (8) (2018) 157–165.
- [17] De Almeida, J.V.; Siqueira, G.L., Experiments on metamaterials for sub-wavelength antenna isolation at PEC boundaries., *Microw. Opt. Technol. Lett.*, (59) (2017) 1420–1423.
- [18] Amjad, I.; Omar, A.S.; Amal, B.; Abdul, B., Metamaterial-based highly isolated MIMO antenna for portable wireless applications. *Electronics*, (7) (2018) 267.
- [19] Jabir, A.H.; Zhang, H.-X.; Abdu, A., Split rectangular loop resonator inspired MIMO monopoles for GSM/LTE/WLAN applications., *J. Commun.*, (14) (2019) in press.
- [20] Ajay Yadav, S.A.; Yadav, R.P., SRR and S-shape slot-loaded triple band-notched UWB antenna., *Int. J. Electron. Commun.* (2017) 192–198.
- [21] Mohanty A, Sahu S., High isolation two-port compact Mimo fractal antenna with wi-max and x-band suppression characteristics., *Int J RF Microwave Comput Aided Eng.*, 30(1) (2020):e22021.
- [22] Deng J-Y, Guo L-X, Liu X-L., An ultrawideband Mimo antenna with high isolation., *IEEE Antennas Wireless Propag Lett.*,(15) (2015)182–5.
- [23] Jehangir SS, Sharawi MS., A miniaturized USB biplanar yagi-like Mimo antenna system., *IEEE Antennas Wireless Propag Lett* (16) (2017) 2320–3.
- [24] Ren J, Hu W, Yin Y, Fan R., Compact printed Mimo antenna for uwb applications., *IEEE Antennas Wirel Propag Lett.*,(13) (2014)1517–20.
- [25] Zhang S, Pedersen GF., Mutual coupling reduction for uwb Mimo antennas with a wideband neutralization line., *IEEE Antennas Wirel Propag Lett.*,(15) (2015)166–9.
- [26] Roshna TK, Deepak U, Mohanan P., Compact uwb Mimo antenna for tridirectional pattern diversity characteristics., *IET Microwaves Antennas Propag.*,11(14) (2017) 2059–65.
- [27] Bilal M, Saleem R, Abbasi HH, Shafique MF, Brown AK., An fss-based nonplanar quad-element uwb-Mimo antenna system., *IEEE Antennas Wirel Propag Lett.*, (16) (2016) 987–90.
- [28] Liu X-L, Wang Z-D, Yin Y-Z, Ren J, Wu J-J., A compact ultrawideband Mimo antenna using qscs for high isolation., *IEEE Antennas Wirel Propag Lett* (13) (2014) 1497–500.
- [29] Roshna T, Deepak U, Sajitha V, Vasudevan K, Mohanan P., A compact uwb Mimo antenna with a reflector to enhance isolation., *IEEE Trans Antennas Propag.*63(4) (2015) 1873–7.
- [30] Alsath MGN, Kanagasabai M., Compact uwb monopole antenna for automotive communications., *IEEE Trans Antennas Propag.*, 63(9) (2015) 4204–8.
- [31] Khan R, Al-Hadi AA, Soh PJ, Isa CMNC, Ali MT, Khan S, et al. Dual polarized antennas with reduced user effects for lte-u Mimo mobile terminals. *AEU Int J Electron Commun.*,(111) (2019) 152880.
- [32] Nirmal PC, Nandgaonkar A, Nalbalwar S, Gupta RK., Compact wideband Mimo antenna for 4g wi-max, WLAN and uwb applications., *AEU Int J Electron Commun.*, (99) (2019) 284–92.
- [33] Garbacz RJ., Modal expansions for resonance scattering phenomena., *Proc IEEE.*,53(8) (1965) 856–64.
- [34] Harrington R, Mautz J., Theory of characteristic modes for conducting bodies., *IEEE Trans Antennas Propag.*,19(5) (1971) 622–8.
- [35] Sultan, K.S.,Abdullah,H. H., Abdallah, E.A.,& El-Hennawy, H. S., Metasurface-based dual-polarized MIMO antenna for 5G smartphones using CMA., *IEEE Access*, (8) (2020) 37250-37264.
- [36] A. C. Suresh and T. S. Reddy, High Isolation With Fork-Shaped Stub In Compact UWB-MIMO Antenna Using CMA, 2021 International Conference on Recent Trends on Electronics, Information, Communication & Technology (RTEICT), (2021) 505-511, doi: 10.1109/RTEICT52294.2021.9574028.
- [37] K. S. Sultan and H. H. Abdullah, Planar UWB MIMO-diversity antenna with dual notch characteristics, *Progress in Electromagnetics Research C*, vol. 93 (2019) 119-129.
- [38] Roshna TK, Deepak U, Mohanan P., Compact uwb Mimo antenna for tridirectional pattern diversity characteristics., *IET Microwaves Antennas Propag.*, 11(14) (2017) 2059–65.
- [39] Maurya NK, Bhattacharya R., Design of compact dual-polarized multiband Mimo antenna using near-field for iot., *AEU Int J Electron Commun* (117) (2020) 153091.
- [40] Tran HH, Hussain N, Le TT., Low-profile wideband circularly polarized Mimo antenna with polarization diversity for WLAN applications., *AEU Int J Electron Commun* (108) (2019) 172–80.
- [41] Azarm B, Nourinia J, Ghobadi C, Majidzadeh M, Hatami N., On the development of a mimo antenna for coupling reduction and WiMAX suppression purposes., *AEU Int J Electron Commun* (99) (2019) 226–35.
- [42] Asutosh Mohanty, Bikash Ranjan Behera, Investigation of 2-port UWB MIMO diversity antenna design using characteristics mode analysis, *AEU Int J Electron Commun.*, (2020) 124- 15361.